Analytical Methods Hot Paper

How to cite: *Angew. Chem. Int. Ed.* **2022,** *61,* e202112346
International Edition: doi.org/10.1002/anie.202112346
German Edition: doi.org/10.1002/ange.202112346

A Lateral Flow Test for *Staphylococcus aureus* in Nasal Mucus Using a New DNAzyme as the Recognition Element

M. Monsur Ali, Ryan Silva, Dawn White, Saeed Mohammadi, Yingfu Li, Alfredo Capretta, and John D. Brennan**

Abstract: *Detection of pathogenic bacteria in complex biological matrices remains a major challenge. Herein, we report the selection and optimization of a new DNAzyme for Staphylococcus aureus (SA) and the use of the DNAzyme to develop a simple lateral flow device (LFD) for detection of SA in nasal mucus. The DNAzyme was generated by in vitro selection using a crude extra/intracellular mixture derived from SA, which could be used directly for simple solution or paper-based fluorescence assays for SA. The DNAzyme was further modified to produce a DNA cleavage fragment that acted as a bridging element to bind DNA-modified gold nanoparticles to the test line of a LFD, producing a simple colorimetric dipstick test. The LFD was evaluated with nasal mucus samples spiked with SA, and demonstrated that SA detection was possible in minutes with minimal sample processing.*

Infection by pathogenic bacteria remains a major health concern and socioeconomical burden.[1] *Staphylococcus aureus* (SA), a gram-positive cocci, is one of the most dangerous and opportunistic human pathogens, causing a variety of infections ranging from benign skin infections to life-threatening septicemia.[2] About 30 % to 50 % of the human population asymptomatically carries this bacteria in the nose, pharynx or on the skin.[3] Being opportunistic, SA infects through injury and surgery, often causing SA bacteremia (SAB),[4] and is also a major food borne pathogen.[5] Moreover, there are emerging antibiotic resistant SA strains, such as methicillin resistant SA (MRSA), that have imposed additional burdens owing to more limited treatment options.[6] Therefore, accurate and convenient detection of SA can play a vital role in preventing the transmission of SA and in following the effectiveness of treatment interventions.

Classical methods involving plate culturing have been successfully used for decades for detecting *S. aureus*.[5a,7] However, while these methods are accurate and sensitive, they require up to 2 days to provide results. More recently, rapid detection techniques such as molecular assays based on polymerase chain reaction and antigen assays utilizing enzyme linked immunoassays (ELISA) have been developed.[7,8] In addition, several rapid tests for SA have been reported, including the MASTASTAPH™ and StaphAurex™ latex agglutination tests, lateral flow tests using antibodies against *S. aureus* cell-wall peptidoglycan and Staphylococcal enterotoxin-A and B, as well as the coagulase test for SA positive blood samples.[9] While these detection methods can produce results in under 1 h, such tests still require extensive sample processing, multiple assay steps, or suffer from poor sensitivity and specificity. Hence, improved assays and rapid tests are needed to allow simple and rapid diagnosis of SA in a manner that is amenable to use in doctor's offices, long-term care facilities or resource limited settings.

The development of bacterial bioassays with RNA-cleaving fluorogenic DNAzymes (RFDs) was introduced a decade ago for *E. coli* detection,[10] and since then, has been utilized for detection of numerous bacteria[11] using both fluorimetric[12] and colorimetric[13] assays. Such RFDs are isolated from random DNA libraries using a crude extra- or intra-cellular mixture (CEM or CIM) of the bacteria of interest, which catalyzes the cleavage of a fluorogenic DNA substrate at a single ribonucleotide embedded in the DNA substrate. This is followed by counterselection using other, related bacteria, where DNAzymes that do not cleave are carried forward to the next round of positive selection. Sequential rounds of positive and counterselection (up to 20) ultimately produce highly active and selective DNAzymes that cleave only in the presence of the intended bacterium.[10]

In this work, we employed the non-directed CEM-CIM selection method[10] to isolate RFDs for *S. aureus*, as shown in Figure 1A. The DNA library, including the relevant oligonucleotide sequences, is provided in Figure S1A in the Supporting Information, while the detailed procedure for the in vitro selection is provided in the Supporting Information and Figure S1B. Briefly, in vitro selection was carried out using a random DNA library (DL) of $\approx 10^{14}$ individual sequences which was ligated to a fluorogenic substrate (FS). This library was first used in a counter-selection round using a mixture of CEM and CIM obtained from methicillin sensitive *S. aureus* (MSSA), *E. coli* and *B. subtilis* to eliminate any non-specific DNAzyme molecules. The uncleaved molecules were then used for positive selection with the CEM-CIM mixture of MRSA, and the

[*] Dr. M. M. Ali, R. Silva, D. White, Dr. S. Mohammadi, Prof. Dr. A. Capretta, Prof. Dr. J. D. Brennan
Biointerfaces Institute, McMaster University
1280 Main Street West, Hamilton, ON L8S 4K1 (Canada)
E-mail: capretta@mcmaster.ca
brennanj@mcmaster.ca
Prof. Dr. Y. Li
Department of Biochemistry and Biomedical Sciences, McMaster University
1280 Main Street West, Hamilton, ON L8S 4K1 (Canada)

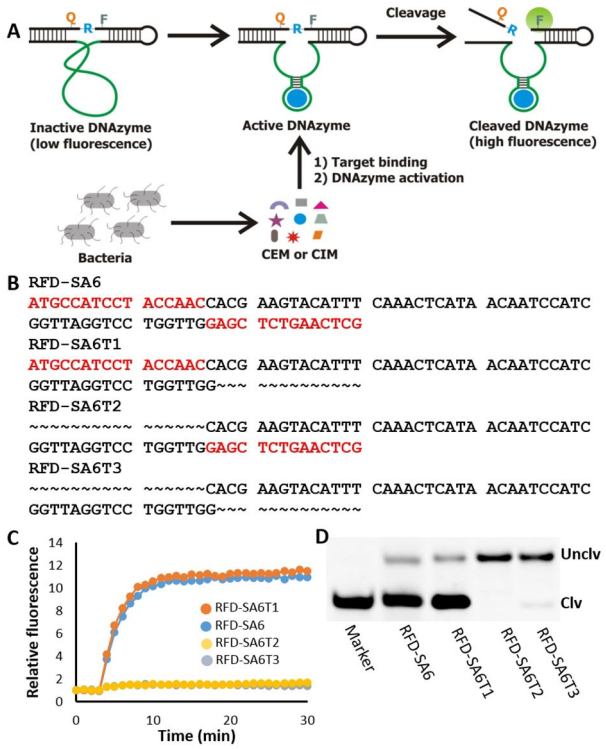

Figure 1. A) Schematic of the DNAzyme cleavage and signalling reaction. The inactive DNAzyme is activated upon binding to the target and cleaves the substrate, producing a high fluorescence signal. B) Sequence truncation studies. RFD-SA6 is the full-length DNAzyme. The red font in both termini denotes the PCR primers for amplification during the selection process. The curved dashed lines in other sequences indicate the deleted nucleotides. C) Cleavage reaction and real time fluorescence signalling of the truncated sequences of B. D) Fluorescence image of 10% dPAGE gel of the reaction mixture of C after a 30 min reaction time.

cleaved molecules were purified, amplified by PCR, and ligated to FS for use in the next round of selection. A significant amount of cleavage product was obtained after 9 rounds of positive selection, with counterselections being carried out every second round to achieve selectivity (Figure S1C).

The population from round 9 was used for deep sequencing and the top twenty sequences (Figure S2) were synthesized and tested for cleavage performance. The results presented in Figure S3 showed that all RFDs cleaved FS in presence of the CEM-CIM of both MRSA and MSSA but did not cleave in presence of multiple other bacteria. These results suggested that the RFDs obtained in selection were activated by a dominant target that was present in both MRSA and MSSA, and thus could not discriminate between these bacteria (Figure S4). Hence, additional rounds of selection or more stringent counterselection steps using a wider range of MSSA subtypes or higher concentrations of MSSA may be needed to achieve high selectivity for MRSA. It may also be necessary to use a different library or a purified target that is unique to MRSA to generate a more selective DNAzyme. Importantly, the DNAzyme still showed high selectivity against many non-SA bacteria, providing a useful molecular recognition element for detection of both methicillin-sensitive and methicillin-resistant SA strains. The RFD denoted as RFD-SA6 had the highest cleavage activity (Figure S3) and was selected for further investigation in this study.

Truncation analysis was carried out to shorten the RFD-SA6 DNAzyme (Figure 1B). Removal of the 3′ primer region had no impact on cleavage, while removal of the 5′ primer region completely eliminated cleavage activity, indicating that the 5′ primer region contained nucleotides essential to the catalytic function of the DNAzyme. One of the truncated versions, denoted as RFD-SA6T1, cleaved the substrate, and generated a fluorescence signal equivalent to the full length DNAzyme, RFD-SA6 (Figure 1C, D). RFD-SA6T1 contained 67 nucleotides and was used in all subsequent experiments. Predicted secondary structures of RFD-SA6 and the truncated RFD-SA6 have been provided in the Supporting Information (Figure S5) and show a substantial change in the secondary structure upon removal of the 5′ primer, which correlates with loss of activity.

RFD-SA6T1 was then evaluated for fluorimetric detection of MRSA and MSSA which was spiked as a CIM-CEM mixture into nasal mucus samples (see details in the SI). As a control we also used unspiked nasal mucus to evaluate the possibility of producing false positive signals from the nasal mucus alone. The results in Figure 2A showed that RFD-SA6T1 produced a high fluorescence signal with the spiked nasal mucus but did not produce any fluorescence signal with nasal mucus alone. This is the first demonstration of an RFD operating in nasal mucus and shows that the RFD can both resist cleavage by nucleases that may be present in these samples, and also retain target-dependent cleavage even in the presence of DNA-binding proteins and other interfering species that may be present in nasal mucus. Additional gel-based data confirmed that the DNAzyme did not cleave in nasal mucus, indicating its resistance to degradation by nucleases in mucus (see Figure S6).

The specificity of RFD-SA6T1 against two strains of MSSA as well as different *Staphylococcus* species and other gram-positive and gram-negative bacteria was then evaluated (Figure 2B), revealing that RFD-SA6T1 selectively produced strong fluorescence responses with all forms of *S. aureus*, but did not respond to any other control bacteria, including several other S*taphylococcu*s species. Corresponding dPAGE images of the cleavage reactions is provided in the Supporting Information (Figure S7).

To test the sensitivity of the RFD-SA6T1, nasal mucus samples spiked with different numbers of MRSA cells were tested and indicated that an RFD-based fluorescence assay could produce a detectable fluorescence signal with 10^4 cells mL^{-1} within 30 min (Figure 2C) and with 10^3 cells mL^{-1} after 80 min (Figure 2D). This detection limit is comparable to that reported for other bacteria-sensitive DNAzymes, including those for *E. coli* (10^4 cells mL^{-1} in 60 min) and *H. pylori* (10^4 cells mL^{-1} in 60 min). Interestingly, the sensitivity of RFD-SA6T1 for detection of MRSA on a paper micro-well plate improved by approximately 10-fold to 10^2 cells mL^{-1} using a 60 min reaction time (Figure 2E, see Supporting Information for details on the

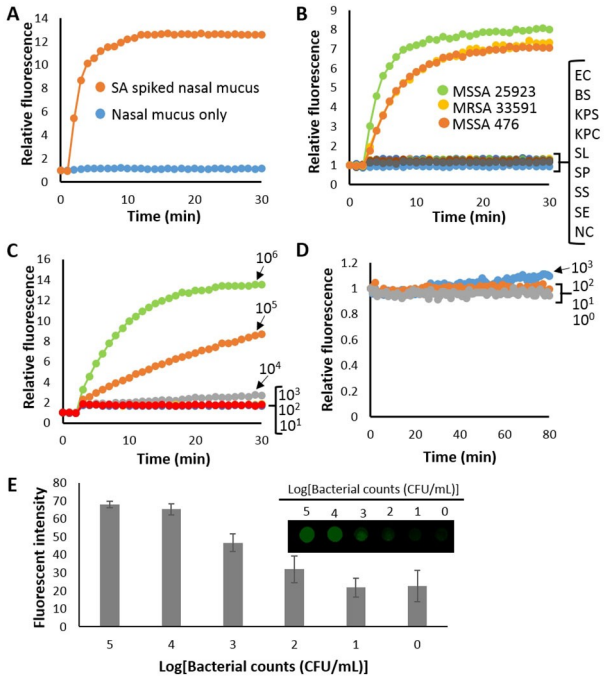

Figure 2. A) Cleavage and fluorescence signalling of RFD-SA6T1 with MRSA spiked into nasal mucus. B) Selectivity of RFD-SA6T1 with different bacterial cell lysates. MSSA: methicillin sensitive *Staphylococcus aureus*, MRSA: methicillin resistant *Staphylococcus aureus*, EC: E. coli, BS: B. subtilis, KPS: drug-sensitive K. pneumoniae, KPC: carbapenem-resistant K. pneumoniae, SL: Staphylococcus lentus, SP: Staphylococcus pasteuri, SS: Staphylococcus saprophyticus, SE: Staphylococcus epidermidis. C) Limit of detection (LOD) obtained using fluorescence signal generation. D) LOD analysis using a lower number of cells and longer reaction time. E) Fluorimetric detection of MRSA on a paper microwell plate.

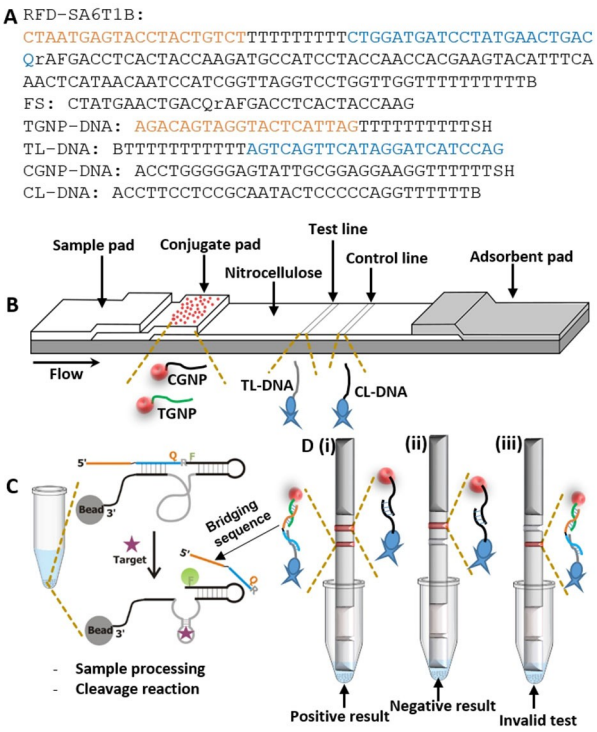

Figure 3. Schematic illustration of the LFD. A) DNA sequences used to develop the LFD. B) Physical description of the LFD showing the specific regions. Sample pad and conjugate pad are assembled at the bottom of a nitrocellulose strip (NCP: 25×5 cm^2). Two different capture DNA oligonucleotides are printed for the test and the control line respectively. An adsorbant pad is attached at the top of the NCP. A mixture of two types of gold nanoparticle with two different oligonucleotides are deposited on the conjugate pad. C) The DNAzyme–bead complex is incubated with the sample to allow the cleavage reaction to occur. The LFD is inserted into the tube such that a portion of the sample pad touches the liquid sample. D) Intrepretation of the results: i) If both the test and the control lines turn into red, the result is considered to be positive. ii) if only the control line turns into red, the result is considered to be negative (no SA in the sample). iii) If only the test line appears, the result is invalid. Details of the device fabrication and assay procedures are provided in the experimental part in the Supporting Information.

production of the paper microwell plate and paper-based assays), which was similar to our previously reported paper-based assays for *E. coli*.[12b,14] Similar improvements in detection limits have been reported and are based on increases in local concentration and reaction rates when moving solution-based assays to a paper surface.[14] Cleavage activity was also tested using intact cells and compared the cleavage results using different lysis conditions. The results showed cleavage activity was retained using intact cells and was similar to that obtained with lysed cells (Figure S8).

To move the DNAzyme-based assay toward a simple and equipment free point-of-care test (POCT) for *S. aureus*, we explored integrating the assay with a lateral flow device (LFD) to produce a simple dipstick test, as shown in Figure 3. To date, there are only a few reports of DNAzyme-based LFDs, all of which are for metal ions.[15] In this work, we utilized the modified version of the cleavage product as a bridging strand.[15b] The LFD was first produced by printing streptavidin-bound biotinylated DNA oligonucleotides, denoted as TL-DNA for the test line and CL-DNA for the control line, onto a nitrocellulose (NC) strip (sequences of all oligonuceoetides used for LFD fabrication are provided in Figure 3A). The NC strip was then attached to a backing card and cut into strips of 4×25 mm size, and a sample pad and a conjugate pad (4×10 mm) were attached along with an adsorbant pad (4×20 mm), as shown in Figure 3B. Finally, two sets of gold nanoparticle (GNP) conjugates were placed on the conjugate pad containing DNA complementary to either the DNAzyme cleavage fragment (test line nanoparticle, TGNP) or the DNA on the control line (named CGNP).

To make the RFD compatible with the LFD assay, the fluorescently-labelled substrate (FS) within the DNAzyme was modified by adding an extended sequence domain in the 5′-end (blue and brown domains in RFD-SA6T1B in Figure 3A) such that the 5′-end of the cleaved fragment of FS binds to the DNA strand on the TGNP and the 3′-end of the cleaved FS binds to the printed DNA strand on the test line, allowing the cleavage fragment to act as a bridging sequence between the TGNP and the DNA printed on the

test line. The 3′-end of RFD-SA6T1 was modified with a biotin to immobilize the DNAzyme onto a streptavidin-modified agarose bead. In this way, the presence of SA in the test solution causes cleavage of the FS within the DNAzyme, releasing the bridging strand into solution, as shown in Figure 3C, while uncleaved DNAzymes remain bound to the beads in solution.

Following the cleavage reaction, the LFD is placed into the test sample to allow the cleaved fragment of FS to travel up the strip and bridge between the TGNP and the test line DNA to form a positive test line along with a positive control line (Figure 3D i). If only the control line is positive the DNAzyme has not cleaved and the test is negative for SA (Figure 3D ii), while the absence of a control line is considered as an invalid result (Figure 3D iii).

Prior to testing the LFD with bacterial samples, we optimized the buffer conditions to produce intense test and control lines when using 20 % nasal mucus and a pre-cleaved product of the DNAzyme as the bridging sequence (blue and brown sequence in RFD-SA6T1B in Figure 3A). 20 % nasal mucus was chosen as higher amounts, such as 50 % nasal mucus, produced high background signals (Figure S9). The details of the optimization experiments are provided in the Supporting Information and the results are provided in Figure S10. The optimal buffer condition was determined to be 1 × selection buffer containing 0.1 % Tween20, which was used as the cleavage/running buffer. In addition, the sample pad was soaked in 0.1 % SDS and dried to aid in blocking of the nitrocellulose surface and improve buffer flow. SDS in the sample pad also prevented non-specific interactions of the bridging sequence with any proteins present in the nasal mucus, avoiding false positive results (Figure S10).

Using the optimized conditions, we next tested whether the DNAzyme could cleave and release the bridging sequence if the DNAzyme was directly immobilized on the LFD. In this case, the DNAzyme immobilized-LFD was directly immersed into the bacterial cell lysate mixed in the cleavage buffer in a tube. It was expected that once the targets along with the buffer moved up the strip, they would cleave the FS to free the bridging sequence to bridge TGNP and TL-DNA to produce a color. However, the results showed only a weak test line (Figure S11 i) when compared with the LFD where the cleavage was first carried out in the test sample followed by the dipping the LFD into the reaction tube (Figure S11 ii), likely owing to insufficient time for DNAzyme cleavage. We therefore used the two step procedure (cleavage then immersion of the LFD) for all subsequent assays. We also note that the F and Q labels were retained on the substrate, as reversal or removal of these labels eliminated cleavage activity (Figure S12), indicating that the labels were required to obtain high cleavage activity.

The specificity of the LFD was first tested with 10^7 cells mL^{-1} of different *Staphylococci.* The cell lysates were spiked into 20 % nasal mucus samples and the cleavage reactions were carried out for 10 min with each of the bacterial samples individually, followed by flowing the sample up the LFD for 20 min. An intense test line was observed on the LFD only for samples containing either MRSA or MSSA but not with other staphylococcus species (Figure 4A), indicating that the LFD maintained specificity and that the nasal mucus samples did not produce false positives or false negatives.

We also tested the sensitivity of the LFD with MRSA-spiked nasal mucus samples. Samples containing different numbers of bacterial cells were prepared as described for the solution-based fluorescence assay in Figure 2C. The cleavage reactions with the bead-immobilized DNAzyme were conducted for 10 min with these samples and the test lines on the LFDs were monitored after 20 min of flow. The results (Figure 4B) revealed that the LFD produced a detectable test line with 10^5 cells mL^{-1}. Use of a longer cleavage reaction time produced background with non-target bacteria (Figure S13). Although the detection limit with the LFD is lower than with the paper-based fluorescence assay, the shorter reaction time allowed the test to be done in 30 min and the signal could be read by eye without any instrument. In addition, the detection limit is below the infectious level of SA in nasal mucus, which is reported to be as high as 10^6 copies per mL.[2d,16] The storage stability of the LFD was also evaluated, and was determined to be at least 6 months when stored desiccated at room temperature (Figure S14).

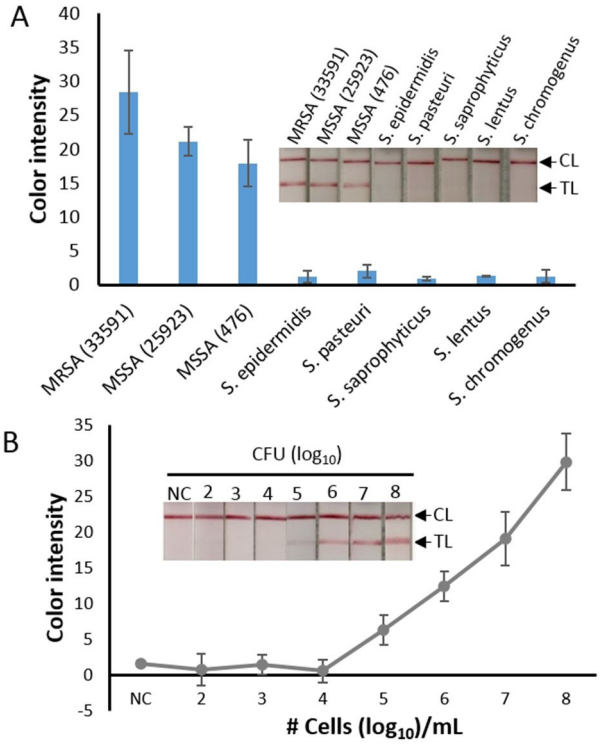

Figure 4. A) Specificity of the LFD against different *Staphylococci.* 33591, 25923 and 476 represent the ATCC numbers of the SA strains. Error bars denote the standard deviation obtained from triplicate experiments for each bacterial species. B) Sensitivity of the LFD to detection of MRSA. The sensitivity was investigated using the MRSA 33591 strain. Error bars represent the standard deviation calculated from triplicate experiments of each dilution of bacterial cells.

Finally, we compared the performance of the DNAzyme-based LFD to Abbot's Alere™ PBP2a lateral flow assay, which has been developed for testing MRSA colonies after plate culture. However, this commercial test produced very strong false positive signals (Figure S15A) with 20% nasal mucus samples and even in pure buffer the limit of detection was only 10^7 CFU mL^{-1} (Figure S15B), and thus this test does not provide performance comparable to the DNAzyme-based LFD.

In summary, we have generated a new DNAzyme for *S. aureus* by in vitro selection and developed solution and paper-based fluorescence assays and a rapid colorimetric LFD assay using the DNAzyme as a recognition element. In all cases the assay performed robustly, even in nasal mucus samples, and could provide test results in a minimally invasive manner in as little as 30 min. The LFD has the additional advantages of being portable and simple to use, and generating a colorimetric readout that can be analyzed without equipment. We believe this work will lay a foundation for developing low-cost portable point-of-care diagnostics using DNAzyme probes for detecting pathogenic bacteria in clinical settings, especially in resource limited areas.

Acknowledgements

Funding for this work was provided by the Ontario Ministry for Research and Innovation (ORF-RE; Grant No. RE07-045) and the Canadian Foundation for Innovation (CFI). JDB holds the Canada Research Chair in Point-of-Care Diagnostics.

Conflict of Interest

The authors declare no conflict of interest.

Keywords: Biosensor · DNAzyme · Lateral flow device · SELEX · Staphylococcus aureus

[1] a) P. N. Fonkwo, *EMBO Rep.* **2008**, S13–17; b) M. Suhrcke, D. Stuckler, J. E. Suk, M. Desai, M. Senek, M. McKee, S. Tsolova, S. Basu, I. Abubakar, P. Hunter, B. Rechel, J. C. Semenza, *PLoS One* **2011**, *6*, e20724; c) N. Uemura, S. Okamoto, S. Yamamoto, N. Matsumura, S. Yamaguchi, M. Yamakido, K. Taniyama, N. Sasaki, R. J. Schlemper, *N. Engl. J. Med.* **2001**, *345*, 784–789.

[2] a) J. Mehraj, W. Witte, M. K. Akmatov, F. Layer, G. Werner, G. Krause, *Curr. Top. Microbiol. Immunol.* **2016**, *398*, 55–58; b) J. R. Fitzgerald, *Infect. Genet. Evol.* **2014**, *21*, 542–547; c) A. Schmidt, S. Bénard, S. Cyr, *Surgery* **2015**, *16*, 428–435; d) A. Sakr, F. Brégeon, J. L. Mège, J. M. Rolain, O. Blin, *Front. Microbiol.* **2018**, *9*, 2419.

[3] a) A. F. Brown, J. M. Leech, T. R. Rogers, R. M. McLoughlin, *Front. Immunol.* **2014**, *4*, 507.

[4] a) C. Shi, Y. Xiao, Q. Zhang, Q. Li, F. Wang, J. Wu, N. Lin, *BMC Infect. Dis.* **2018**, *18*, 508; b) H. Asgeirsson, A. Thalme, O. Weiland, *Infect. Dis.* **2018**, *50*, 175–192; c) C. Gudiol, G. Cuervo, E. Shaw, M. Pujol, J. Carratalà, *Expert Opin. Pharmacother.* **2017**, *18*, 1947–1963; d) C. K. Naber, *Clin. Infect. Dis.* **2009**, *48*, S231-7.

[5] a) M. Rubab, H. M. Shahbaz, A. N. Olaimat, D. H. Oh, *Biosens. Bioelectron.* **2018**, *105*, 49–57; b) L. Marquez, T. H. Koy, C. R. Baker, J. Graf, E. M. Whaley, J. R. Campbell, *Infect. Control. Hosp. Epidemiol.* **2018**, 1–2; c) S. M. Puah, J. A. M. A. Tan, C. H. Chew, K. H. Chua, *J. Food Sci.* **2018**, *83*, 2337–2342.

[6] a) S. Lakhundi, K. Zhang, *Clin. Microbiol. Rev.* **2018**, *31*, e00020-18; b) A. S. Lee, H. D. Lencastre, J. Garau, J. Kluytmans, S. Malhotra-Kumar, A. Peschel, S. Harbarth, *Nat. Rev. Dis. Primers* **2018**, *4*, 18033.

[7] V. Templier, Y. Roupioz, *J. Appl. Microbiol.* **2017**, *123*, 1056–1067.

[8] a) C. Zi, D. Zeng, N. Ling, J. Dai, F. Xue, Y. Jiang, B. Li, *BMC Microbiol.* **2018**, *18*, 132; b) M. O. Lara, T. C. Lucas, E. Kalapothakis, R. L. Thomasini, C. J. Machado, *Rev. Soc. Bras. Med. Trop.* **2018**, *51*, 528–532; c) W. Surasa, H. H. Peter, B. D. Kenneth, D. A. Lea, *Diagn. Microbiol. Infect. Dis.* **2013**, *75*, 28–36.

[9] a) M. Zschöck, A. Nesseler, I. Sudarwanto, *J. Appl. Microbiol.* **2005**, *98*, 450–455; b) J. Asante, B. A. Hetsa, D. G. Amoako, A. L. K. Abia, L. A. Bester, S. Y. Essack, *Antibiotics* **2021**, *10*, 198; c) L. Essers, K. Radebold, *J. Clin. Microbiol.* **1980**, *12*, 641–643; d) C. J. Papasian, B. Garrison, *Diagn. Microbiol. Infect. Dis.* **1999**, *33*, 201–203.

[10] a) M. M. Ali, S. D. Aguirre, H. Lazim, Y. Li, *Angew. Chem. Int. Ed.* **2011**, *50*, 3751–3754; *Angew. Chem.* **2011**, *123*, 3835–3838.

[11] a) Z. Shen, Z. Wu, D. Chang, W. Zhang, K. Tram, C. Lee, P. Kim, B. J. Salena, Y. Li, *Angew. Chem. Int. Ed.* **2016**, *55*, 2431–2434; *Angew. Chem.* **2016**, *128*, 2477–2480; b) M. M. Ali, M. Wolfe, K. Tram, J. Gu, C. D. M. Filipe, Y. Li, J. D. Brennan, *Angew. Chem. Int. Ed.* **2019**, *58*, 9907–9911; *Angew. Chem.* **2019**, *131*, 10012–10016; c) M. M. Ali, A. Slepenkin, E. Peterson, W. Zhao, *ChemBioChem* **2019**, *20*, 906–910; d) M. Rothenbroker, E. M. McConnell, J. Gu, M. L. Urbanus, S. E. Samani, A. W. Ensminger, C. D. M. Filipe, Y. Li, *Angew. Chem. Int. Ed.* **2021**, *60*, 4782–4788; *Angew. Chem.* **2021**, *133*, 4832–4838; e) E. M. McConnell, I. Cozma, Q. Mou, J. D. Brennan, Y. Lu, Y. Li, *Chem. Soc. Rev.* **2021**, *50*, 8954–8994.

[12] a) S. D. Aguirre, M. M. Ali, B. J. Salena, Y. Li, *Biomol. Eng.* **2013**, *3*, 563–577; b) M. M. Ali, C. L. Brown, S. Jahanshahi-Anbuhi, Y. Li, J. D. Brennan, *Sci. Rep.* **2017**, *7*, 12335; c) C. Ting, W. Yongcheng, Z. Ling-Li, W. Ye, T. Ye, H. A. John, W. A. David, Z. Ying-Lin, Z. Xin-Xiang, *Chem. Commun.* **2019**, *55*, 7358–7361.

[13] K. Tram, P. Kanda, B. J. Salena, S. Huan, Y. Li, *Angew. Chem. Int. Ed.* **2014**, *53*, 12799–12802; *Angew. Chem.* **2014**, *126*, 13013–13016.

[14] M. Liu, C. Y. Hui, Q. Zhang, J. Gu, B. Kannan, S. Jahanshahi-Anbuhi, C. D. M. Filipe, J. D. Brennan, Y. Li, *Angew. Chem. Int. Ed.* **2016**, *55*, 2709–2713; *Angew. Chem.* **2016**, *128*, 2759–2763.

[15] a) D. Mazumdar, J. Liu, G. Lu, J. Zhou, Y. Lu, *Chem. Commun.* **2010**, *46*, 1416–1418; b) Z. Fang, J. Huang, P. Lie, Z. Xiao, C. Ouyang, Q. Wu, Y. Wu, G. Liu, L. Zeng, *Chem. Commun.* **2010**, *46*, 9043–9045; c) J. Chen, X. Zhou, L. Zeng, *Chem. Commun.* **2013**, *49*, 984–986.

[16] a) P. Verhoeven, F. Grattard, A. Carricajo, B. Pozzetto, P. Berthelot, *J. Clin. Microbiol.* **2010**, *48*, 4242–4244.

Manuscript received: September 10, 2021
Accepted manuscript online: November 23, 2021
Version of record online: December 2, 2021